DOI: 10.61782/fa.2025.0731

FORUM ACUSTICUM
EURONOISE 2025

RECONSTRUCTION OF RADIATED ACOUSTIC FIELDS USING 3D LASER VIBROMETRY AND FEM SIMULATION: A COMPARATIVE STUDY OF INTERPOLATION APPROACHES

Paweł Nieradka[1*] **Matheus Veloso**[1] **Jakub Jóska**[1]
Bartosz Chmielewski[1] **Michał Kozupa**[2] **Grzegorz Kmita**[2]
[1] KFB Acoustics sp. z o. o., Acoustic Research and Innovation Center, Oławska 8, 55-040 Domasław, Poland
[2] Hitachi Energy Research, Pawia 7, 31-154 Kraków, Poland

ABSTRACT

This study presents a methodology for reconstructing the radiated acoustic field of a box-like structure using laser vibrometry (LV) scanning and finite element method (FEM) simulation. The complex vibration velocities in all three directions were measured on the surface of a 3D noise source. These velocities were then converted into normal velocity boundary conditions for FEM simulations to predict the radiated noise. Due to the absence of predefined CAD geometry for the analyzed object, data from discrete points were interpolated to form a complete 3D radiating surface. Different approaches were tested to address these challenges. The study compares sound power levels, directivity plots, and the effort required for post-processing data for each approach. Future research will involve comparing the predicted sound power levels and directivity plots with results obtained from other methods.

Keywords: *acoustic radiation, acoustic field, laser vibrometry, interpolation*

1. INTRODUCTION

The theoretical prediction of sound radiation based on the distribution of vibration velocity on a surface is a well-established topic in the literature [1]. When only space-averaged RMS velocity values are available, a simplified models based on radiation efficiency can be applied [2]. To compute radiation efficiency the mechanical and geometrical parameters of radiating surface are required, which is the main disadvantage of this method. If the full complex velocity field (including phase relationships) of the radiating surface is determined, this distribution can be used as a boundary condition in numerical simulations, such as FEM and BEM, to predict radiated sound power. With the advancement of laser vibrometry, this approach has been increasingly used for predicting the radiated power of building partitions [3] and other sound-radiating surfaces, such as compressor walls [4]. Additionally, sound power estimated from vibration velocity distributions has been utilized to predict the sound insulation performance of building elements [5]. Since measurements provide vibration velocity data at discrete points, defining a continuous velocity distribution is necessary for modeling vibrating structures. Various interpolation techniques are employed for this purpose, and the accuracy of radiated sound power prediction depends on the chosen interpolation method. Wurzinger applied linear interpolation combined with a projection of measurement points onto a CAD model using a single linear transformation [6]. Gaussian process regression (GPR) interpolation has also been tested, demonstrating higher accuracy in extrapolating field values at domain boundaries, especially at low frequencies and with a limited number of measurement points [7]. In this study, we employ linear interpolation, which does not require advanced mathematical modeling and is the fastest and simplest to implement. It is considered appropriate when a sufficiently dense grid of measurement points is

[*] ***Corresponding author**: p.nieradka@kfb-acoustics.com*

used, with particular attention to domain boundaries, but it can slightly underestimate real sound power [7]. Although various interpolation techniques have been explored, the literature lacks a comprehensive comparative analysis of different linear interpolation methods (2D vs. 3D) and their specific impact on the accuracy of acoustic field predictions. This paper aims to address this gap by providing a detailed evaluation of these methods and their influence on the predicted sound radiation. To achieve this, vibration velocity measurements were conducted on a test object using a laser vibrometer, followed by an acoustic simulation utilizing the measured velocity data.

2. MEASUREMENTS

Vibration measurements were taken in a semi-anechoic chamber equipped with a Polytec Robovib system with 3D laser vibrometer in the research laboratory of KFB Acoustics, ARIC (Acoustic Research and Innovation Center). Robotic arm KUKA KR C4 equipped with set of 3 scanning vibrometer heads was programmed in Robovib system to move around the object reaching 12 measurement positions (Fig. 1).

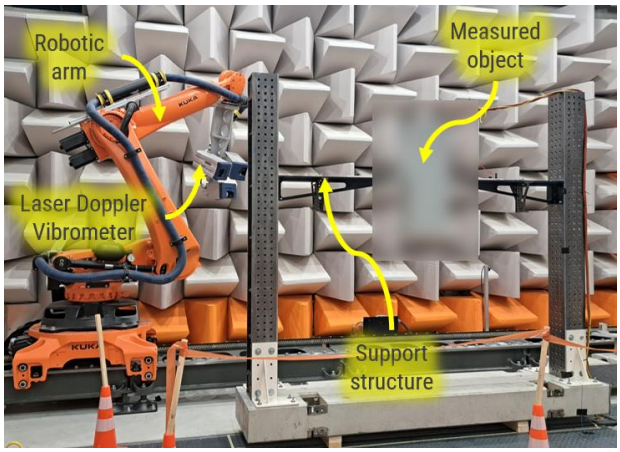

Figure 1. Laser vibrometry measurement set-up.

Due to confidential reasons the precise identification of the device under test (DUT) is not provided here. Predefined CAD geometry files of the object were not used during the measurements. The cloud of points representing the DUT was collected in-situ by using built-in geometry laser scanner to produce a single 3D object (Fig. 2a). The total number of measured points was equal to 14056. The approximate size of the object was 340 mm x 180 mm x 840 mm (Length x Width x Height). That results in an average of 1.4 measurement points per cm^2. The investigated object could be set to generate tonal noise at 50 Hz, 100 Hz, 200 Hz or 400 Hz. For each frequency the 3D vibrational scan of the object was performed by sampling structure's complex (phase and amplitude) response from all measurement points (Fig. 2b).

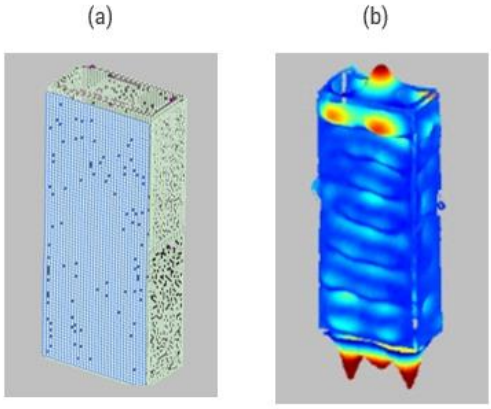

Figure 2. (a) Measured cloud of points representing the DUT's geometry, (b) Example snapshot of experimental vibrational field.

3. FEM MODEL

The development of the FEM model was conducted in Comsol Multiphysics and took place in five stages: i) creation of the geometry (box representing the DUT and sphere for sound power evaluation); ii) creation of the interpolation functions related to the experimental measurements; iii) definition of air as the domain used in the sphere; iv) imposition of the normal velocity boundary conditions and Perfectly Matched Boundary Condition (PMB); v) development of the numerical model mesh.
Regarding the mesh used, it is important to highlight that convergence analyses were performed to define the maximum size of the elements. The mesh was defined separately for the box and the sphere, considering 500 elements per wavelength and 6 elements per wavelength, respectively.

3.1 Preparing geometry

In this work two methods were used to develop the DUT's geometry used in the numerical model: i) creation of the geometry within Comsol, considering the dimensions of the rectangular box (height, width and thickness); ii) use of the coordinates (cloud of points) obtained through the vibrometer. The cloud of points was converted to an *.stl

file with the help of Matlab function alphaShape (Fig. 3) and then imported in Comsol. In Fig. 4, the complete model (box and sphere for evaluating sound power) with the mesh already defined is visualized.

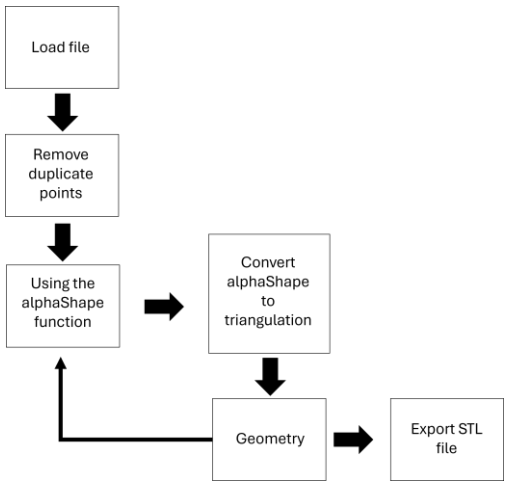

Figure 3. Flowchart of geometry development through the experimentally obtained cloud of points.

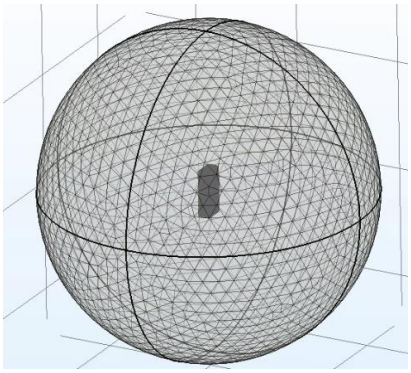

Figure 4. Mesh of the FEM model.

In Fig. 5 one can see the normal direction coordinate variability (standard deviation of approximately 12 mm for each face). Those coordinates were kept unchanged for the "cloud of points" geometry and set constant for simple cuboid geometry.

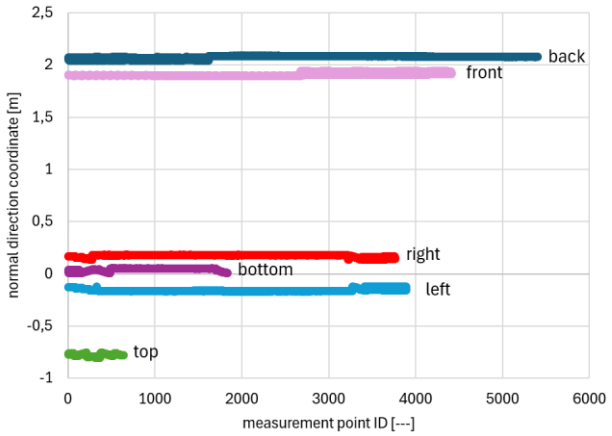

Figure 5. Normal direction coordinate variability for each measurement point.

3.2 Velocity field interpolation

Two independent sets of linear interpolation functions were prepared. First set consisted of 2D interpolations functions $f_{2D,\,i,\,j,\,k}$ based only on the data from individual faces. Second set consisted of "global" 3D interpolation functions $f_{3D,\,i,\,j}$ based on all data points. Index i represents the real and imaginary parts: i = {real; imag}, index j represents the direction: j = {x, y, z}, and index k represent the DUT's walls: k = {top, bottom, left, right, front, back}. The extrapolation procedure is required in case of using 2D interpolation functions because it is impossible to measure DUT's response exactly at edges and corners. Therefore, there is always a narrow region of unknown velocity field near the boundaries of each interpolated face. Constant interpolation was employed, which uses the value from the closest mesh element.

3.3 Normal velocity

Experimentally obtained complex velocities in all 3 directions converted to linear interpolation functions were assigned to FEM model as a normal velocity boundary condition. This boundary condition provided the normal component of the velocity vector depending on the surface orientation of each geometrical component. Two cases were considered: Approach A and Approach B. In approach A the geometry recreated from cloud of points was used and six (representing each DUT's face) 3D interpolation functions (representing real and imaginary parts of x, y and z velocity components) were assigned to all model's boundaries (Fig. 6).

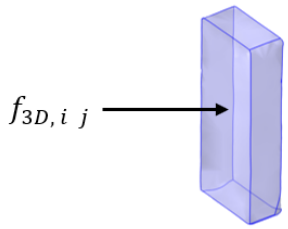

Figure 6. Geometry and the set of normal velocity boundary conditions for approach A. Notice irregular shape of the box recreated from the cloud of points. Index *i* stands for real and imaginary part, index *j* stands for x, y and z direction.

In approach B (Fig. 7) the simplified cuboid geometry was used and each DUT's face (front, back, left, right, top and bottom) was assigned with individual set of six 2D interpolation functions (representing real and imaginary parts of x, y and z velocity components on particular wall). Therefore, the total number of thirty-six different 2D interpolation functions were used in approach B. Assigned velocities were directly compared with experimental results to validate the proper application of boundary conditions.

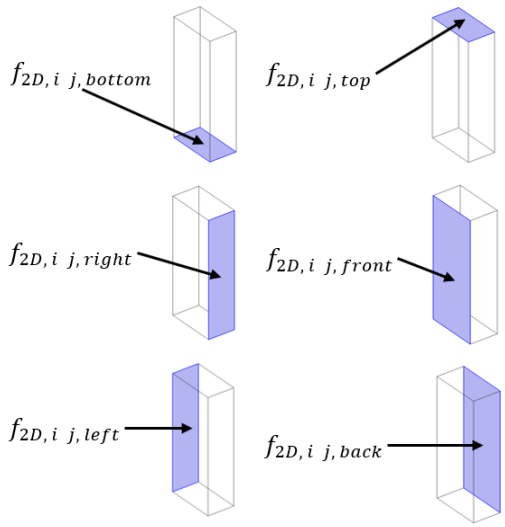

Figure 7. Geometry and the set of normal velocity boundary conditions for approach B. The object is modelled as a perfect cuboid. Index *i* stands for real and imaginary part, index *j* stands for x, y and z direction.

3.4 Sound radiation

For the analysis of sound radiation, it was assumed that the vibrating box was empty, with no domain assigned to its interior. The integration of sound intensity was performed over a spherical surface enclosing the box. The sphere radius was equal to 3 m, and air was considered the medium. Additionally, the PMB boundary condition was imposed to prevent sound reflections in the medium. The acoustic power was determined by integrating the sound intensity over the sphere's surface.

4. RESULTS

In this section, the results of acoustic power and directivity obtained using methods A and B will be compared. The time spent preparing the model using method B was only 1.5 times longer than preparing the model using method A. However, this ratio may significantly increase for other geometries with more complex shapes. In such cases, recreating from scratch simplified geometry as in method B may become suboptimal, cumbersome, or even impossible.

4.1 Sound power level

The sound power determined by methods A and B is shown in Fig. 8. As can be seen, sound power level of the DUT increases with frequency. There is a very good agreement between results from approach A and B. The biggest difference of 3 dB is observed at 100 Hz.

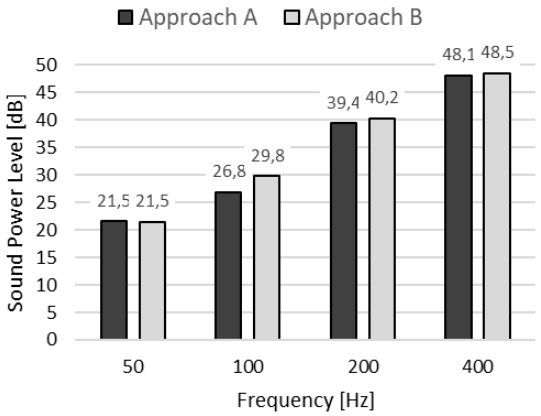

Figure 8. Sound power level of the DUT obtained from approach A and B at each frequency.

4.2 Directivity

Sound pressure level distribution for each frequency and cut plane was obtained. Example result for yz cut plane is shown in Fig. 9. The sound source directivity for the xy, xz and yz planes is shown in Fig. 10, 11 and 12, respectively. The dB values on directivity plots are scaled so they represent sound power levels associated with specific direction. The analyzed source is omnidirectional in the yz plane for all frequencies, but it's directivity pattern become more complicated in the xz and yz plane at higher frequencies. Directivity patterns reveal the difference in results from approach A and B at 100 Hz, where lower levels were obtained for approach A. For other frequencies very similar results are observed from both approaches. The difference in results could be explained by the fact, that different interpolation data sets were used in both approaches (see 2D vs 3D interpolation description at section 3.2) and 100 Hz data set seems to be most sensitive. Therefore, reconstructing exactly the same (or similar) velocity fields from both methods is not always possible.

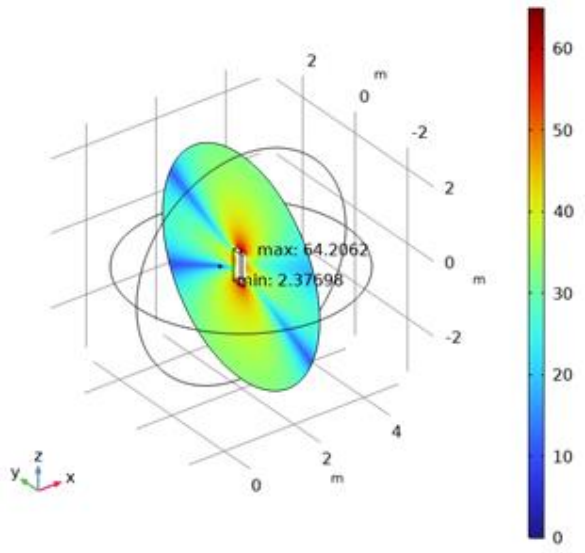

Figure 9. Example result of total sound pressure distribution, yz cut plane.

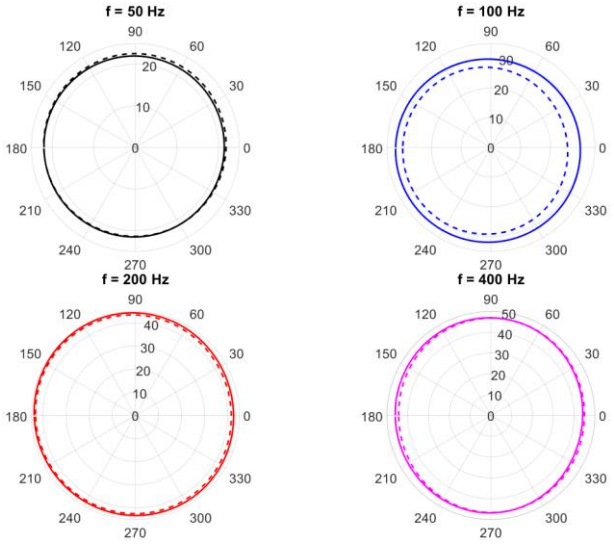

Figure 10. Directivity plot, xy cut plane. Dashed line: approach "A", solid line: approach "B".

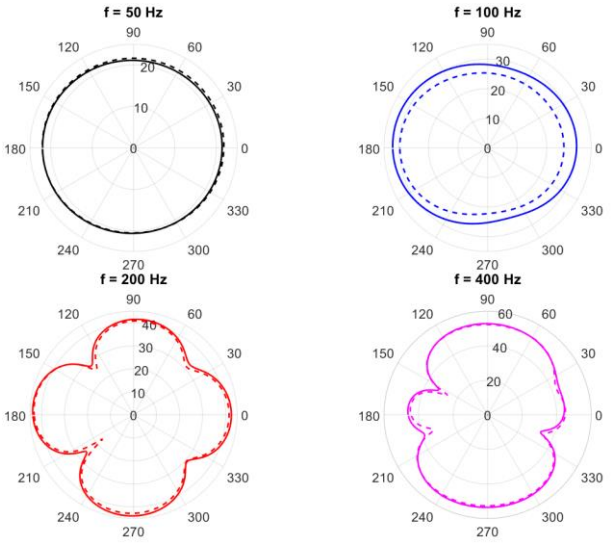

Figure 11. Directivity plot, xz cut plane. Dashed line: approach "A", solid line: approach "B".

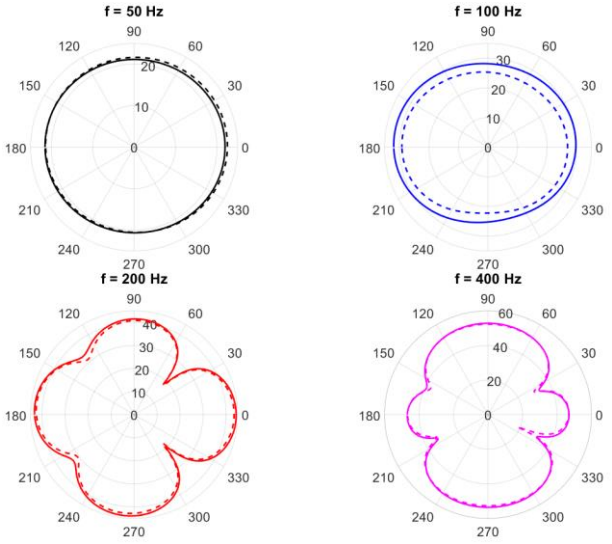

Figure 12. Directivity plot, yz cut plane. Dashed line: approach "A", solid line: approach "B".

5. SUMMARY

In this paper, two different velocity field interpolation approaches were compared. Very good agreement was observed in predicting both radiated power and directivity for 50 Hz, 200 Hz, and 400 Hz. The biggest difference of 3 dB was observed at 100 Hz. This might be attributed to the use of different interpolation data sets in each approach, which can lead to different interpolation results. For example, 2D interpolation requires data extrapolation towards the edges, while 3D interpolation does not. Additionally, the 3D interpolation result is affected by the vibrational field of each wall, while 2D interpolation functions are affected only by the field of separate walls. Consequently, it is not always feasible to reconstruct identical (or similar) velocity fields using both methods. Additional analyses are required to fully understand the reasons for observed differences. Approaches A and B with the current geometry are similar in terms of time spent on model preparation. Nevertheless, the partly automatized geometry preparation present in method A could be very advantageous when dealing with more complicated geometries. Next research steps will involve conducting DUT's sound power level measurements by using different methods.

6. REFERENCES

[1] S. M. Kirkup: "Computational solution of the acoustic field surrounding a baffled panel by the Rayleigh integral method.", *Applied mathematical modelling*, vol. 18, no. 7, pp. 403–407, 1994.

[2] D. Fritze, S. Marburg, and H. J. Hardtke: "Estimation of radiated sound power: A case study on common approximation methods.", *Acta Acustica united with Acustica*, vol. 95, no. 5, pp. 833–842, 2009.

[3] N. B. Roozen, L. Labelle, M. Rychtáriková, and C. Glorieux: "Determining radiated sound power of building structures by means of laser Doppler vibrometry.", *Journal of Sound and Vibration*, vol. 346, no. 1, pp. 81–99, 2015.

[4] D. E. Montgomery, R. L. West, and R. A. Burdisso: "Acoustic radiation prediction of a compressor housing from three-dimensional experimental spatial dynamics modeling.", *Applied Acoustics*, vol. 47, no. 2, pp. 165–185, 1996.

[5] N.B Roozen, Q. Leclere, D. Urbán, T. M. Echenagucia, P. Block, M. Rychtáriková, and C. Glorieux: "Assessment of the airborne sound insulation from mobility vibration measurements; a hybrid experimental numerical approach.", *Journal of Sound and Vibration*, vol. 432, no. 1, pp. 680–698, 2018.

[6] A. Wurzinger, et al.: "Experimental prediction method of free-field sound emissions using the boundary element method and laser scanning vibrometry.", *Acoustics MDPI*, vol. 6, no. 1, pp. 65–82, 2024.

[7] A Wurzinger, et al., "Prediction of vibro-acoustic sound emissions based on mapped structural dynamics.", in *INTER-NOISE and NOISE-CON Congress and Conference Proc.*, (Nantes, France), pp. 8251–8260, 2024.